

Gamma Rays from Thermal Neutron Capture in Cl, V, Mn, and Co†

O. A. WASSON, K. J. WETZEL, AND C. K. BOCKELMAN

Electron Accelerator Laboratory, Yale University, New Haven, Connecticut

(Received 3 August 1964)

The high-energy γ rays ($E_\gamma > 5$ MeV) emitted in thermal-neutron capture by Cl, V, Mn, and Co have been observed with 20-keV resolution using a single lithium-drifted germanium detector and paraffin-moderated Pu-Be neutrons. The previously reported ground-state γ rays in Mn and V are found to contain primary transitions to the first excited states near 20-keV excitation. In addition, previously unreported lines in all four elements have been observed; most of these have been identified as primary transitions to levels known from (d, p) studies. Little correlation between the reduced γ -ray strengths I_γ/E_γ^2 from the (n, γ) reaction, and the relative transition strengths $(2J+1)S$ from the (d, p) reaction, is observed in Co and V.

INTRODUCTION

THE study of the spectrum of γ rays which follow the capture of a nucleon is, in principle, an extremely useful tool for the investigation of nuclear structure. The high-energy end of the γ -ray spectrum is composed of radiations which relate highly excited nuclear states, presently describable only in statistical terms, to levels low in excitation which lie in the region where theories of nuclear structure are beginning to illuminate the observations. If the mechanism of capture could be ascertained, analysis of the properties of individual capture lines would offer partial information on the wave functions of highly excited states in the form of electromagnetic matrix elements which connect these states to the better known low-lying states. Even without detailed knowledge of the capture mechanism, considerable knowledge of spins and parities of nuclear states rather high in excitation has been derived from directional correlations measured for both proton- and neutron-capture γ rays. However, in each case the experiments have been limited by the relatively low-energy resolution of NaI detectors. In the special case of thermal neutron capture, the intense fluxes available from reactors have permitted experimenters the use of magnetic spectrometers as well as crystal diffraction spectrometers, with which resolutions of better than 1% are available.¹ Only with the magnetic spectrometers has it been possible to observe in detail individual high-energy transitions in the spectra of medium and heavy elements. Such data have been especially useful in determining the size and variation of $E1$ matrix elements. However, the high resolution of these instruments is obtained at the cost of a very low efficiency, of the order of 10^{-7} or less. Thus even with thermal neutrons it is necessary to use the $\sim 5\%$ efficiency of NaI spectrometers to do coincidence experiments.

Within the last year the development of Li-drifted Ge detectors² has made available a γ -ray spectrometer which offers resolutions better than 10 keV with effi-

ciencies of the order of 10^{-3} . This instrument promises to revolutionize the entire field of γ -ray spectroscopy. In the present paper, such a detector is used with ~ 20 keV resolution to obtain thermal neutron-capture γ -ray spectra in the energy region of 5 to 8 MeV for Cl, Mn, V, and Co at considerably better resolutions than heretofore published. The chlorine spectrum has been well measured earlier,³⁻⁶ and found to consist of several well-spaced lines of good intensity. This particular spectrum served as a good test of the linearity and efficiency variation of the detector. In the more complex spectra of V, Mn, and Co a number of hitherto unresolved γ rays are reported. In particular, for both V⁵² and Mn⁵⁶ the initial transitions to the ground state and first excited state, which differ by about 20 keV in each case, are separated for the first time. On the plausible assumption that all the γ rays observed are initial transitions, much of the new data can be identified as terminating on levels previously measured in high-resolution (d, p) studies. However, in a few cases the inferred levels lie in regions previously not explored, in that they were obscured in the charged particle work.

Although coincidence studies would have been extremely valuable, the neutron flux available in the present experiment was too low to permit such measurements.

EXPERIMENTAL DETAILS

The experimental geometry is shown in Fig. 1. The γ rays following thermal neutron capture in the sample are detected by a Li-drifted germanium detector. The thermal neutrons are produced by moderating in a paraffin barrel the high-energy neutrons emitted by 5 Pu-Be neutron sources, each emitting 1×10^6 neutrons per sec. The $1\frac{1}{2}$ -in. bismuth plug attenuates by approximately 95% the flux of 4.43-MeV γ rays which is also emitted by the sources. The samples whose capture

³ G. A. Bartholomew and L. A. Higgs, Atomic Energy of Canada, Ltd. Report 669, 1958 (unpublished).

⁴ L. V. Groshev, A. M. Demidov, V. N. Lutsenko, and V. I. Pelekov, *Atlas of γ -Ray Spectra from Radiative Capture of Thermal Neutrons* (Pergamon Press, Inc., New York, 1959).

⁵ L. V. Groshev, A. M. Demidov, and V. N. Lutsenko, *Izv. Akad. Nauk SSSR, Ser. Fiz.* **24**, 833 (1960).

⁶ J. E. Draper and C. O. Bostrom, *Nucl. Phys.* **47**, 108 (1963).

† Research supported in part by the U. S. Atomic Energy Commission under contract AT(30-1)2726.

¹ G. A. Bartholomew, J. W. Knowles, and G. E. Lee-Whiting, *Rept. Progr. Phys.* **23**, 453 (1960).

² G. T. Ewan and A. J. Tavendale, *Nucl. Instr. Methods* **26**, 183 (1964).

γ-ray spectra were desired were placed around the bottom and sides of the detector chamber so that a solid angle of $\sim 3.8\pi$ sr was subtended at the detector. This technique permits the measurement of intense high-energy γ rays for samples with large capture cross sections.

The detector was processed from a 2 cm×2 cm×1 cm thick piece of 10 Ω-cm gallium-doped germanium following the procedures described by Ewan and Tavendale² and by Liles.⁷ Six days of pulsed drifting in a fluorocarbon bath at an average power level of 30 W was sufficient to achieve a depletion depth of 6 mm as indicated by capacity measurements as well as by the copper stain technique. After compensating at 0°C for 6 h at 1500 V and then re-etching, the detector, with an active volume of 2.5 cm² by 0.6 cm thick, was kept under vacuum at liquid-nitrogen temperature.

The signals from the detector were amplified and shaped by an Ortec Model 101 preamplifier followed by an Ortec Model 201 amplifier. Peak broadening due to pulse pileup was reduced by insertion of an 0.8 μsec clip at the amplifier input. The pulses were recorded in a 400 channel pulse-height analyzer. The precision pulser incorporated in the amplifier was employed to determine the linearity of the system to a 0.1% accuracy. An electronic noise level equivalent to 10 keV was characteristic of the system.

The detector was operated at a bias of 650 V which produced a minimum peak width [full width at half-maximum (FWHM)] of 10 keV for the full energy peak from the Cs 660-keV γ ray. At lower bias voltages the peaks were broadened by lower charge collection efficiency while at higher bias voltages the noise contribution from leakage currents was dominant. The peak widths were found to be a function of the γ-ray energy.

For cobalt the two-photon escape peak width increased with energy up to 21 keV (FWHM) at $E_\gamma = 7.2$ MeV, while for manganese, measured subsequently, an increase to 25 keV at 7.0 MeV was observed. Before the vanadium run, the detector was recompensated and re-etched, resulting in improved performance as indicated by the use of a bias of 725 V. The width of the full energy 660-keV peak was again 10 keV but peak width increased with energy only to 17 keV at 7.2-MeV γ-ray energy. While no explanation is certain, in view of the increased resolution and more symmetric peak shapes for the vanadium spectra, it is thought that detector collection efficiency, which is a function of bias voltage among other things, might be the dominant factor in this variation of peak width and peak shape with incident γ-ray energy.

For γ-ray energies in the region of interest in the present experiment, the detector response is dominated by the two-photon escape peak following pair production. Peaks associated with single-photon escape and full

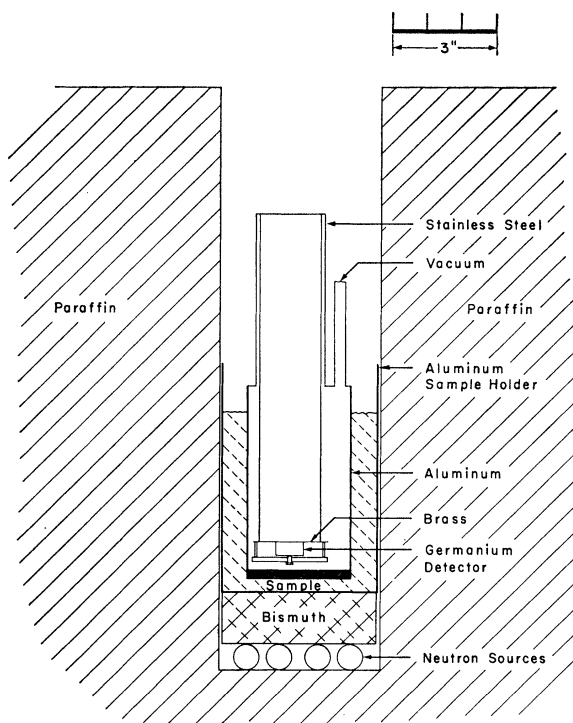


FIG. 1. Scale drawing of experimental geometry.

absorption are much smaller. Under the conditions of the present experiment such peaks are superimposed on a smoothly rising continuum composed of the tails produced by Compton scattering of γ rays in the Ge detector, by pair-produced electrons and positrons escaping from the active volume of the detector, and by incomplete charge collection. Since no monoenergetic pure high-energy γ-ray source is available, the detector response was inferred from the background measurement shown in Fig. 2, which shows a spectrum taken with no sample in place. The double- and single-escape peaks, Compton continuum, and the total absorption peak from the $\text{Be}^9(\alpha, n\gamma)\text{C}^{12}$ 4.43-MeV γ ray produced in the Pu-Be source are readily observed. It is seen that the total-absorption and single-photon escape peak areas are each less than 5% of the double-photon escape peak area for this γ ray. The 85-keV width of the peaks from the 4.43-MeV Pu-Be γ ray is due to the kinematics of the $\text{Be}^9(\alpha, n\gamma)\text{C}^{12}$ reaction and not to the detector. Also seen are peaks produced by neutron capture γ rays from copper and aluminum in the detector chamber.

The 4.43-MeV γ ray, in addition to the strong 2.23 hydrogen capture line, obscures γ rays from the sample having energies less than 4.5 MeV. Also contributing to this spectrum are the effects of the scattering of the MeV neutrons by the detector and the germanium capture γ rays. However, any germanium capture γ rays are too weak to be seen in the presence of the more intense backgrounds. It is uncertain how much of the

⁷ Barry J. Liles, Yale University Electron Accelerator Laboratory Internal Report (unpublished).

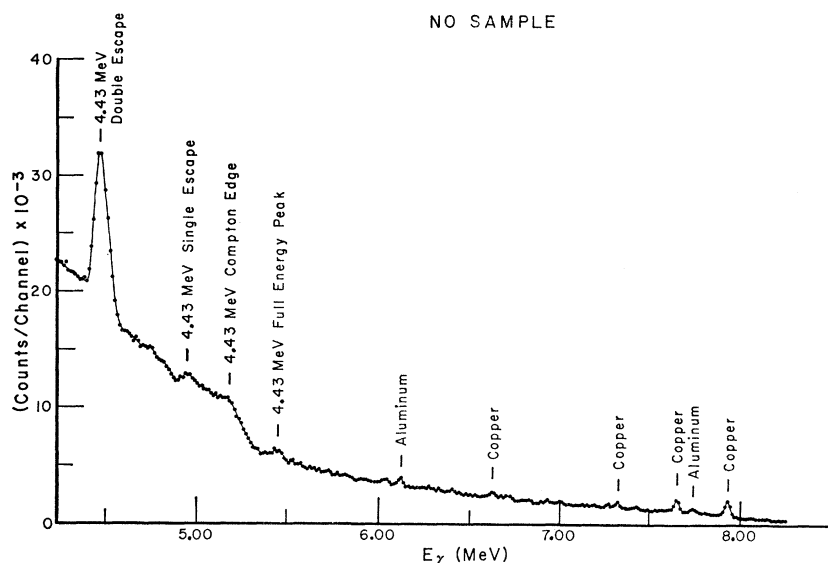


FIG. 2. The γ -ray spectrum observed with a gain of ~ 14 keV/channel with no sample in place. Note the energy scale associates the full γ -ray energy with the 2-photon escape peak.

smooth part of the spectrum is due to neutron scattering and how much is due to the tails of capture γ rays.

The no-sample spectrum serves to determine the energies but not the intensities of background peaks in the sample spectra because the insertion of the sample changes the neutron flux distribution. Since some of the samples absorbed as much as 80% of the incident thermal neutron flux, no direct sample-in sample-out background subtraction was possible. However, sample-in runs were in general followed by sample-out runs of approximately the same duration with the same electronic gain. The appearance of the high-energy copper and aluminum lines in the sample-in spectra aided in the assessment of the background contributions.

In order to obtain the relative detector efficiency as a function of γ -ray energy, a comparison was made with previously measured intensities. In particular, the areas under the more intense two-photon escape peaks in the Cl and V spectra were compared to the earlier measured intensities^{3,4} (summing areas for γ rays not resolved earlier). The disagreement among the earlier measurements prevents an accurate assessment of the shape of the efficiency curve. In lieu of better knowledge, a simple linear fit over the range 5–8 MeV was used. This yields for the relative detector efficiency ϵ_γ in this experimental configuration (normalized to unity at 5 MeV)

$$\epsilon_\gamma = 1.00 + (0.20 \pm 0.02)[5.00 - E_\gamma \text{ (MeV)}]. \quad (1)$$

Using this relative efficiency, the relative gamma-ray intensity I_γ is determined by

$$I_\gamma = A_\gamma / \epsilon_\gamma, \quad (2)$$

where A_γ is the measured area of the double-photon escape peak. In the tables I_γ is expressed in photons/100 neutron captures by normalizing the sum of the measured intensities to the sum of the absolute intensities

determined by other experiments for the same energy interval.

The absolute energy calibration of this experiment was limited to 1% accuracy; however, γ -ray energies were determined to within ± 10 keV by using the results of other experiments. The energies of the levels of the residual nuclei studied are all quite well known from magnetic-analysis measurements of (d,p) spectra. Previous measurements of the γ -ray spectra, obtained with resolutions of the order of 1%,^{3,4} have shown that the observed high-energy γ rays have the energies expected for initial transitions originating at an excitation corresponding to the neutron binding energy and terminating on one of the known low-lying levels. Accepting this type of identification, several of the strong lines in each of the spectra of the present experiment have been identified with initial transitions to known (d,p) levels. The γ -ray energy for these lines was obtained by adding the binding energy of the deuteron, 2.226 MeV, to the measured (d,p) Q value. Using this calibration together with the measured linearity of the electronics system, it was found that the majority of the remaining lines have energies which correspond to other known levels. Exceptions are discussed individually.

Although the energy of the double-photon escape peak is 1.022 MeV less than the energy of the incident γ ray, the energy scale used in all figures in this paper labels the double-photon escape peaks with the energy of the γ ray. Whenever peak energies are mentioned, they will always refer to the incident γ -ray energy.

EXPERIMENTAL RESULTS

Chlorine

The sample consisted of commercial grade CCl_4 contained in a thin-walled aluminum can. The sample

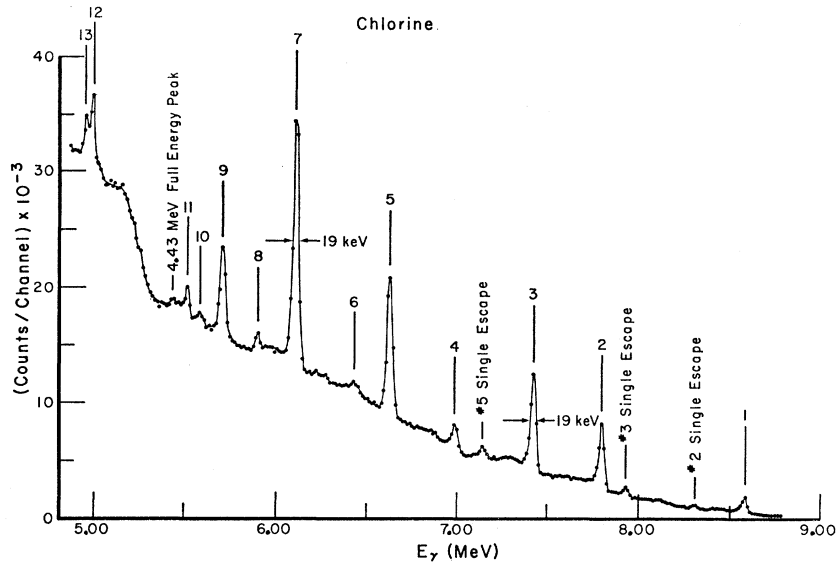


FIG. 3. Chlorine γ -ray spectrum observed with a gain of ~ 14 keV/channel.

thickness was ~ 2.6 g/cm² yielding a value of $n\sigma \sim 12$ where n is the number of Cl³⁵ nuclei/cm² and σ is the thermal-neutron absorption cross section of Cl³⁵. The capture γ -ray spectrum obtained with an electronic gain of 14 keV/channel is shown in Fig. 3. In addition to the numbered peaks, which are identified as two-photon escape peaks, weak single-photon escape peaks are also observed and are so labeled in the figure. The single-escape peak associated with peak 7 coincides with peak 5. The peak widths were ~ 19 keV (FWHM) for this sample. All peaks except No. 6 can be identified as primary transitions from the capturing state to known low-lying levels in Cl³⁶.

The energies and intensities of the observed γ rays are listed in Table I. The energy calibration was deter-

mined by adding 2.226 MeV to the corresponding Q values⁸ measured in the (d,p) experiments of Hoogenboom *et al.*⁹ for the γ rays marked with an “*.” The remaining γ -ray energies, as determined from a linear fit to this standard, agree within experimental error to the (d,p) excitation energies and demonstrate the linearity of the system. It is noted that four of the γ rays were unreported in previous (n,γ) measurements^{3,4,6,10} while the identification of the remaining transitions agrees with that of the earlier investigators. The γ -ray intensities as measured by these investigators are also listed in the table. The origin of peak 6 is undetermined. It is not present in the no-sample measurements and does not correspond to a primary transition to a known level in Cl³⁶.

Since all peaks had typical widths, there was no suggestion of unresolved peaks and no higher gain runs were undertaken. Due to the large background, weak peaks with energies less than 5.3 MeV were probably not observed.

Vanadium

The vanadium sample consisted of 99.9% purity V₂O₅ powder with an effective thermal neutron thickness of $n\sigma \sim 0.2$. The thermal capture γ -ray spectra as observed with an electronic gain of 3.5 keV/channel are shown in Figs. 4, 5, and 6. These spectra cover the energy interval $4.8 \leq E_\gamma \leq 7.4$ MeV.

The thermal γ -ray spectrum for $E_\gamma > 500$ keV^{4,5} and for $E_\gamma > 1.1$ MeV³ has been observed with $\sim 1\%$ resolu-

TABLE I. Chlorine γ -ray energies and intensities. The asterisks in column 1 indicate the γ rays used for energy calibration using a binding energy, B_n , of 8.568 MeV from Refs. 8 and 9. Column 3 lists the energies of the states populated by the γ -ray transitions as compared to the states measured by the (d,p) experiments of Ref. 9 and listed in column 4. The sum of the intensities of the 13 γ rays observed in this experiment and listed in column 5 was normalized to 70 photons per 100 neutron captures following Refs. 4, 3, and 6.

Peak number	E_γ (MeV)	$B_n - E_\gamma$	E_{ex} (MeV)	I_γ (photons/100 captures)			
				Present exp.	Ref. 4	Ref. 3	Ref. 6
1*	8.586	0.000	0.000	2.6	3.1	1.4	2.3
2*	7.797	0.789	0.789	7.0	8.2	7	8.4
3*	7.423	1.163	1.163	10.1	12.3	6	9.9
4	6.986	1.600	1.599	2.4	2.5	2	2.7
5	6.632	1.954	1.954	13.2	13.6	9	13.0
(6)	6.437	2.149		<1			
7*	6.114	2.472	2.472	20.7	25.3	14	21
8	5.898	2.688	2.679	1.0			
9*	5.718	2.868	2.868	5.6	6.1	6	7.7
10	5.581	3.005	3.000	0.8	2.3	3	<2
11	5.510	3.076	3.103	1.9			
12	5.000	3.586	3.606	3.0	4.2	9	5.4
13	4.950	3.636	3.640	1.5			

⁸ Except for vanadium, all (d,p) ground-state Q values have been corrected to account for the revised Po²¹⁰ α -particle energy standard of 5.3042 ± 0.0016 MeV, as reported by A. Sperduto and W. W. Buechner, in Proceedings of the Vienna Conference on Nuclidic Masses (to be published).

⁹ A. M. Hoogenboom, E. Kashy, and W. W. Buechner, Phys. Rev. **128**, 305 (1962).

¹⁰ J. E. Draper and A. A. Fleischer, Phys. Rev. **122**, 1585 (1961).

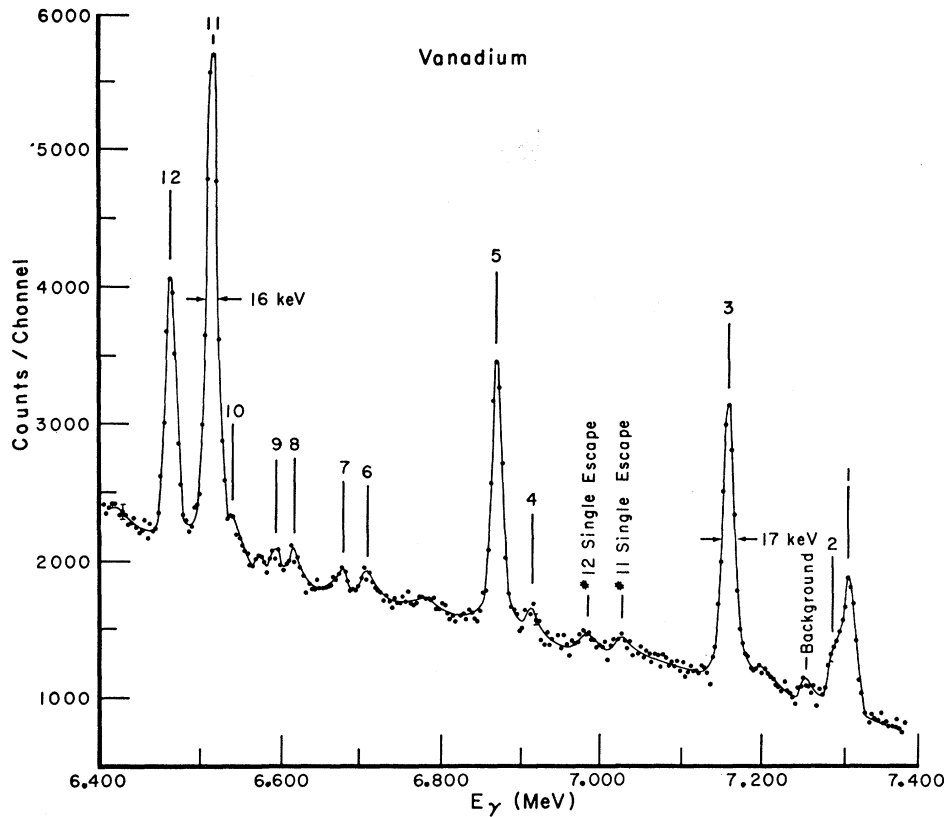


FIG. 4. Vanadium γ -ray spectrum observed with a gain of ~ 3.5 keV/channel for $6.30 \leq E_\gamma \leq 7.40$ MeV.

tion with magnetic spectrometers. Single and coincident thermal spectra have been measured for separated isotopic samples of both V^{51} and V^{52} with NaI crystals.¹¹

A more detailed determination of the low-lying V^{52} levels has been made by White *et al.*¹² using NaI for coincidence studies and a bent-crystal spectrometer for

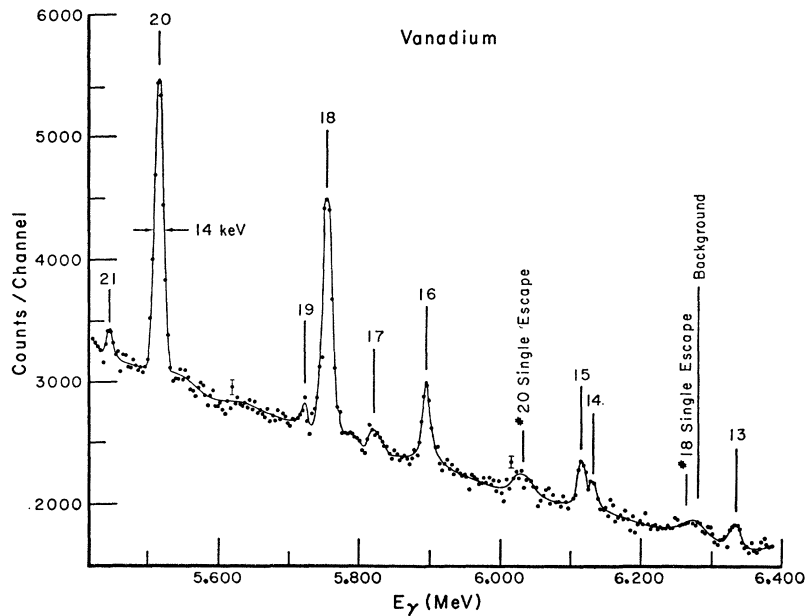


FIG. 5. Vanadium γ -ray spectrum observed with a gain of ~ 3.5 keV/channel for $5.40 \leq E_\gamma \leq 6.40$ MeV.

¹¹ J. E. Schwäger, Phys. Rev. 121, 562 and 569 (1961).

¹² D. H. White, W. John, and B. G. Saunders, in Argonne National Laboratory Report 6797, p. 79, 1963 (unpublished).

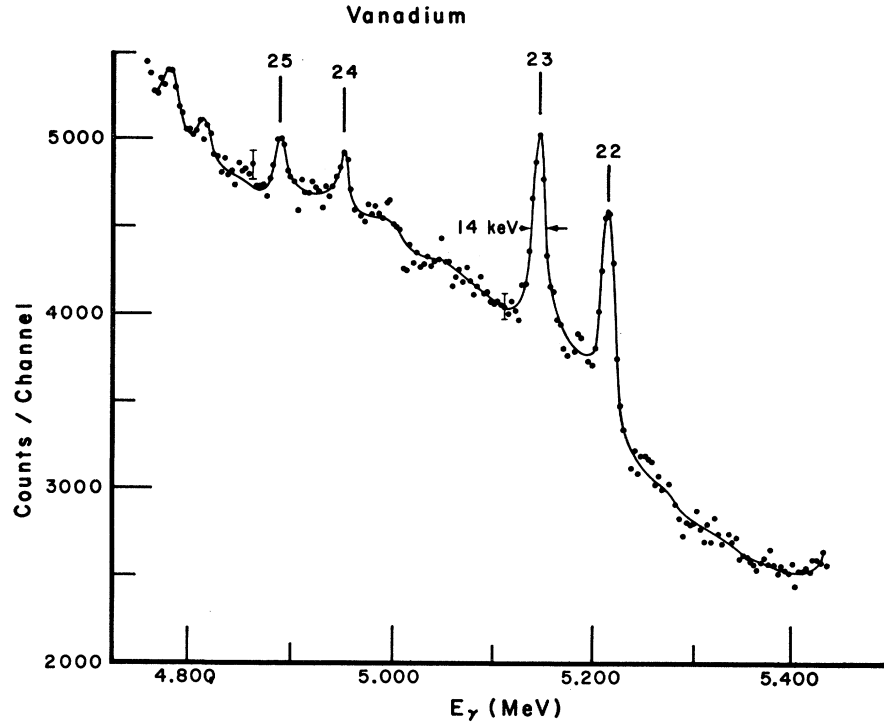


FIG. 6. Vanadium γ -ray spectrum observed with a gain of ~ 3.5 keV/channel for $4.85 \leq E_\gamma \leq 5.45$ MeV.

precise energy measurement of the decay γ rays. The authors of the latter work infer states at 17.0 and 22.8 keV as well as at 141.5 and 147.8 keV.

The energy levels in V^{52} populated in the (d,p) experiments of the MIT¹³ and Copenhagen¹⁴ groups are shown in Fig. 7. The values of l_n , the orbital angular momentum of the captured neutron, as determined from the MIT angular distributions, are listed in the figure. The doublets of White *et al.* at 20 and 146 keV are not observed in this (d,p) work. On the basis of the measured thermal-capture cross section and the parameters of the nearest positive energy resonances, it appears¹⁵ that the thermal neutron capture proceeds through both possible spin states ($3^-, 4^-$).

The list of the observed γ -ray energies and "absolute" intensities is shown in Table II. The sum of the 25 γ -ray intensities has been normalized to 64 photons per 100 neutron captures following Refs. 3 and 4. The energy calibration was determined from the (d,p) levels indicated by asterisks in Table II and a neutron binding energy of 7.306 MeV,¹⁴ assuming peak 1 to be the ground-state transition. The good fit which results indicates that peak 1 is indeed the ground-state transition. Sixteen of the γ rays have energies consistent with being primary transitions to known (d,p) levels and are shown in the level diagram of Fig. 7. The γ rays of this group which have been previously unreported are in-

TABLE II. Vanadium γ -ray energies and intensities. The parentheses indicate the peak numbers of uncertain origin which are tentatively assigned to $V^{50}(n,\gamma)$. The peaks used for energy calibration are indicated by asterisks in column 1, using a neutron binding energy, B_n , of 7.306 MeV from Ref. 14. The fourth column lists the excitation energies determined from the (d,p) experiments of Refs. 13 and 14 which are associated with the indicated γ -ray transitions. The γ -ray intensities listed in columns 5-7 are in units of photons per 100 neutron captures. The sum of the 25 intensities observed in this experiment has been normalized to 64 photons per 100 neutron captures, the average for this energy interval of the intensities of Refs. 3 and 4.

Peak number	E_γ (MeV)	$B_n - E_\gamma$	E_{ex} (MeV)	I_γ (photons/100 captures)		
				Present exp.	Ref. 4	Ref. 3
1*	7.306	0.000	0.000	3.5	5.7	7
2	7.285	0.019	0.020	1.7		
3	7.156	0.150	0.146	7.9		
(4)	6.917	0.389		0.4		10
5*	6.875	0.431	0.431	6.0	8	8
(6)	6.709	0.579		0.5		
(7)	6.682	0.624		0.4		
(8)	6.618	0.688		0.5		
(9)	6.594	0.712		0.3		
(10)	6.538	0.768		0.5		
11*	6.519	0.787	0.787	11.2	12	16
12*	6.465	0.841	0.841	5.8	7	...
(13)	6.338	0.968		0.6		
(14)	6.136	1.170		0.5		
(15)	6.118	1.188		0.4		
16*	5.900	1.406	1.406	1.8	2	2
17	5.822	1.484	1.484	0.6		
18*	5.756	1.550	1.550	5.8	5.6	7
19	5.727	1.579	1.577	0.2		
20*	5.520	1.786	1.786	6.0	7.2	8
21	5.450	1.856	1.827	0.5		
22*	5.222	2.084	2.084	3.4	6.5	5
23*	5.154	2.152	2.152	3.4		
24*	4.957	2.349	2.347	0.7		
25*	4.894	2.412	2.412	0.9	0.8	2

¹³ H. A. Enge, MIT Laboratory of Nuclear Science Progress Report, p. 98, 1960 (unpublished).

¹⁴ J. H. Bjerregaard, P. F. Dahl, O. Hansen, and G. Sidenius, Nucl. Phys. 51, 641 (1964).

¹⁵ F. W. K. Firk, J. E. Lynn, and M. C. Moxon, Proc. Phys. Soc. (London) 82, 477 (1963).

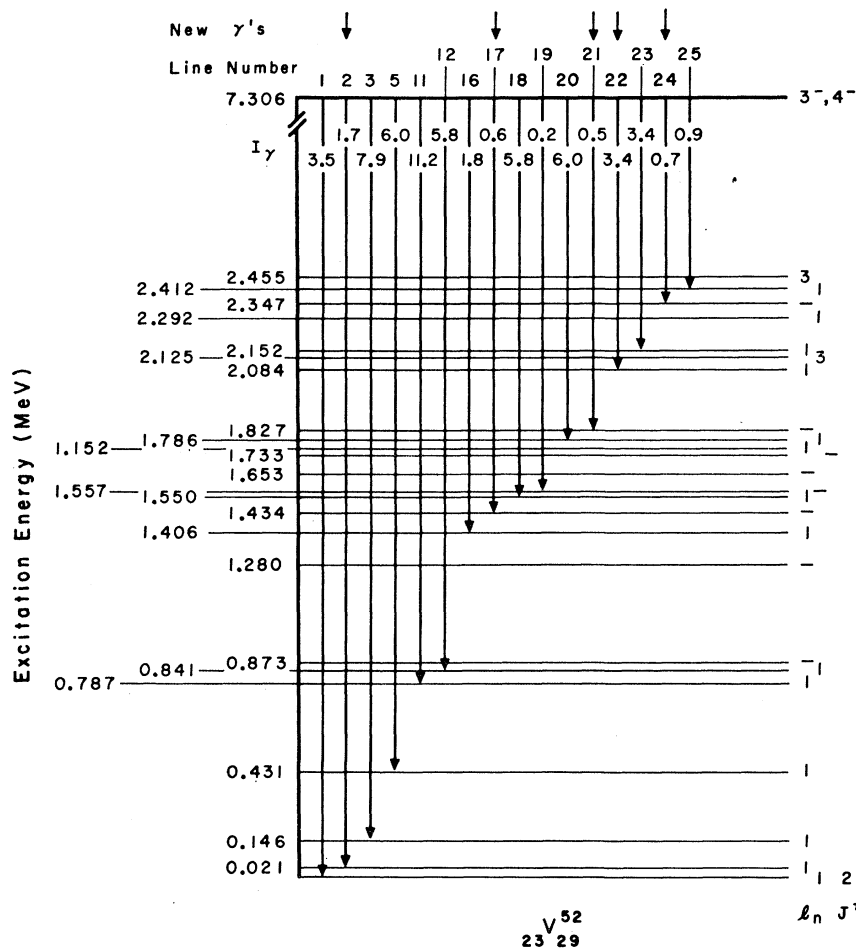


FIG. 7. The V^{52} energy level diagram. The excitation energies are determined from Refs. 13 and 14. The orbital angular momentum l_n of the captured neutron is shown on the right of the diagram. The vertical lines indicate the γ -ray transitions observed in this experiment. The new or previously unresolved γ rays are noted by arrows at the top of the diagram. Intensities I_γ are given in photons/100 neutron captures. The sum of the 25 γ -ray intensities has been normalized to 64 photons/100 neutron captures following Refs. 3 and 4.

dictated by arrows. The remaining 9 weak transitions, which contain less than 6% of the total intensity of the

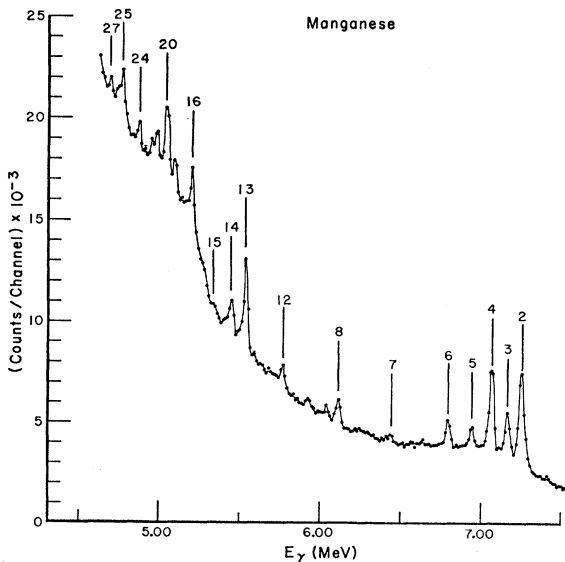


FIG. 8. Manganese γ -ray spectrum observed with a gain of 14 keV/channel.

26 transitions, are enclosed in parentheses in Table II but are not included in Fig. 7. It is assumed that these γ 's are from $V^{50}(n,\gamma)$. The V^{50} isotope may possibly contribute 10% to the total V capture cross section,¹⁶ in which case V^{51} γ -ray transitions would be expected to be observed. However, little is known of the V^{51} γ rays in this energy region.

As is evident by the shape of peak 1, this highest energy peak contains more than one component. Increasing the gain to 1.7 keV/channel did not resolve the peak completely. Due to the uncertainty in the shape of the background under the peak, as well as the finite detector resolution, the limited statistics, and possible small electronic gain shifts, no unique unfolding was obtained. Using peak 3 as the detector line shape, it was possible to unfold the peak into both two components and three components, with the three-component fit being slightly better. The two-component fit showed that $(65 \pm 5)\%$ of the total peak intensity is to the ground state while $(35 \pm 5)\%$ goes to a level at 19 ± 3 keV excitation. The three-component fit, which gives $(65 \pm 5)\%$ of the intensity to the ground state, (25

¹⁶ *Nuclear Data Sheets*, compiled by K. Way *et al.* (Printing and Publishing Office, National Academy of Science—National Research Council, Washington 25, D. C., 1963), NRC 20418.

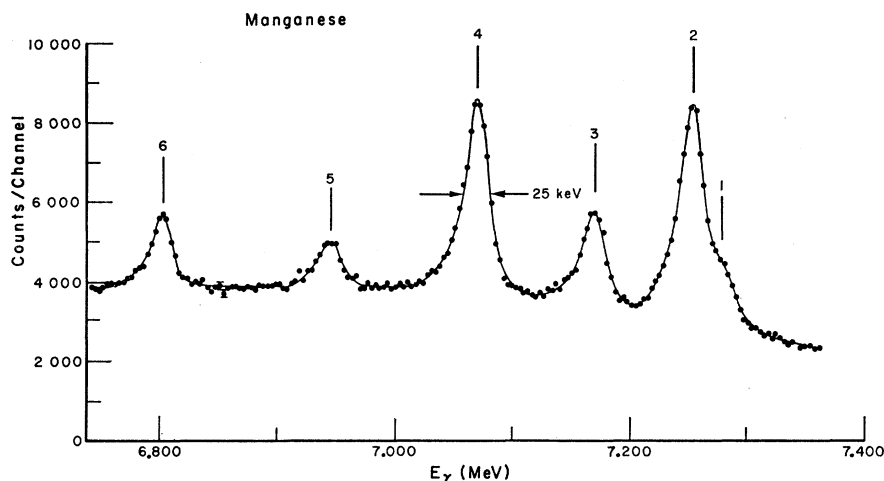


FIG. 9. Manganese γ -ray spectrum observed with a gain of ~ 3.5 keV/channel for $6.70 \leq E_\gamma \leq 7.40$ MeV.

$\pm 5\%$ to a 16 ± 3 keV level, and $(10 \pm 5)\%$ to a 22 ± 3 keV level, would show that primary transitions populate the three states of White *et al.*'s level diagram.¹⁷ The two-component results are included in Fig. 7 and Table II.

Manganese

The sample consisted of 99.9% pure finely powdered manganese contained in the thin-walled aluminum can. The sample thickness corresponded to a value of $n\sigma \sim 1.6$. The γ -ray spectrum obtained with an electronic gain of 14 keV/channel is shown in Fig. 8. Examination of this spectrum suggested incomplete resolution, so the experiment was repeated with a gain of 3.5 keV/channel. These spectra are shown in Figs. 9, 10, and 11. The shape of the highest energy peak at 7.28

MeV suggests the existence of more than one γ ray. Using the shape of peak 4 for the detector line shape, it was possible to unfold the high-energy peak into a doublet separated by 25 ± 3 keV, with $(22 \pm 5)\%$ of the total peak intensity due to transition 1.

The energies and intensities of the γ rays observed in this experiment are shown in Table III. This experiment reveals the existence of 27 γ rays while earlier investigations^{3,4} had detected only 16 transitions in this energy region. Again the identification of the peaks was accomplished by assuming them to be two-quantum escape peaks, due to initial transitions to levels observed in the (d,p) reaction.^{14,18} Using a neutron binding energy of 7.278 MeV³ for the ground-state transition, the energies of 24 of the γ rays corresponded in this manner to known (d,p) levels within the experimental errors

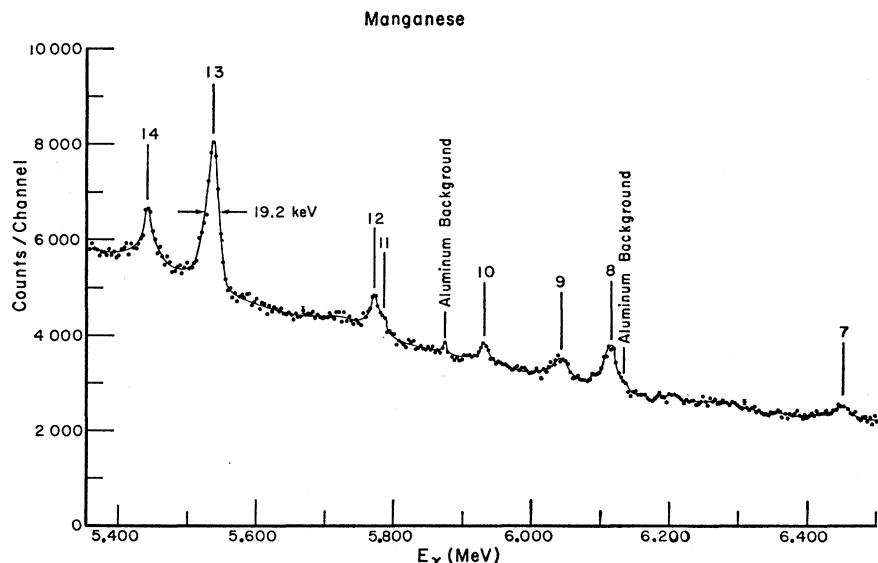


FIG. 10. Manganese γ -ray spectrum observed with a gain of ~ 3.5 keV/channel for $5.35 \leq E_\gamma \leq 6.50$ MeV.

¹⁷ We are grateful to G. G. Slaughter, who has supplied us with preliminary data from similar measurements on V at Oak Ridge. The ground-state and 20-keV levels are clearly resolved, with the ground-state transition being approximately 20% more intense.

¹⁸ J. W. Green, A. J. Smith, W. W. Buechner, and M. Mazari, Phys. Rev. 108, 841 (1957).

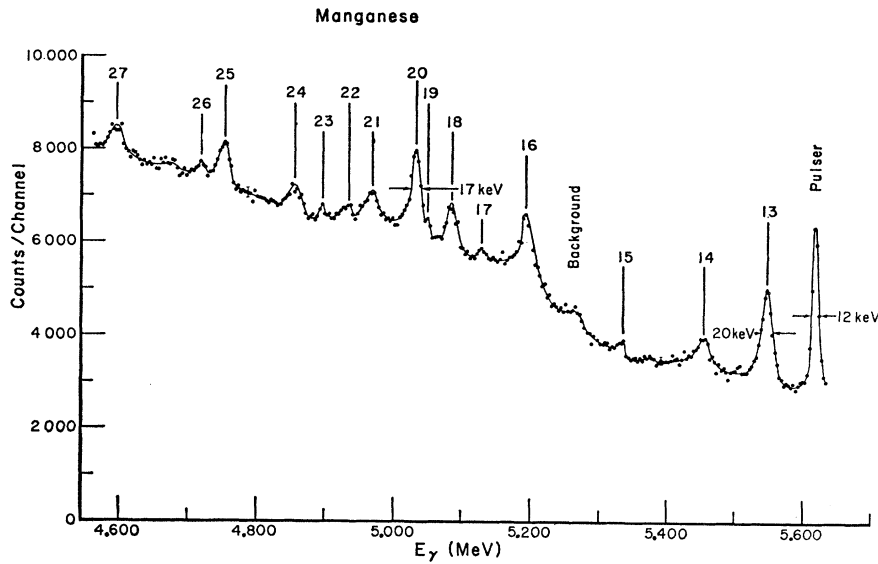


FIG. 11. Manganese γ -ray spectrum observed with a gain of ~ 3.5 keV/channel for $4.60 \leq E_\gamma \leq 5.60$ MeV.

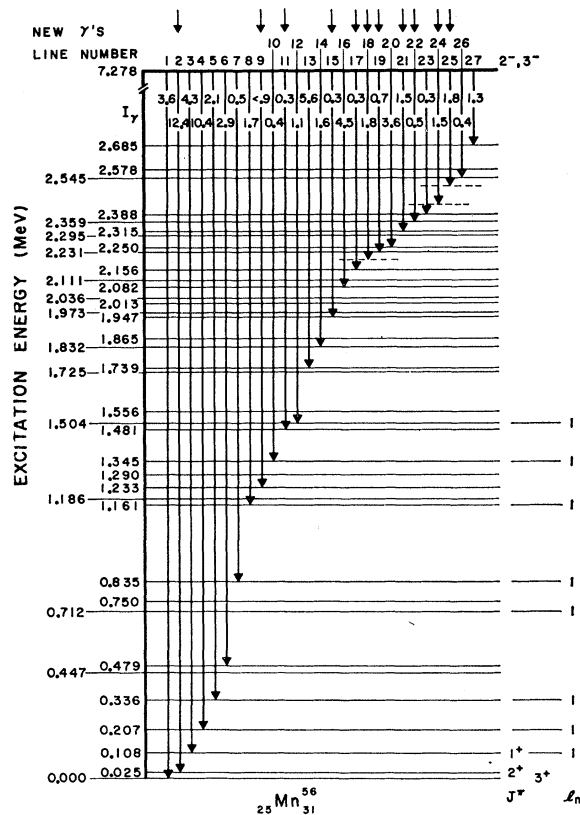


FIG. 12. The M^{56} energy level diagram. The excitation energies are taken from Refs. 14 and 18. The orbital angular momenta are taken from Ref. 20. The neutron binding energy is derived from Ref. 8. The vertical lines indicate the γ -ray transitions observed in this experiment. The transitions previously unresolved or unobserved are noted by arrows at the top of the figure. Intensities, I_γ , are given in photons/100 neutron captures. The sum of the 27 γ -ray intensities has been normalized to 66 photons per 100 neutron captures following Ref. 4.

(± 15 keV). If γ rays 17, 23, and 24 are initial transitions, they terminate on levels not hitherto observed. However, it should be noted that the excitation region corresponding to lines 23 and 24 was obscured by a

TABLE III. Manganese γ -ray energies and intensities. The peaks indicated by an asterisk were used for energy calibration using a neutron binding energy, B_n , of 7.278 MeV from Refs. 8, 14, and 18. Column 4 lists the energy levels populated by the γ -ray transitions as observed in the (d,p) experiments of Ref. 18 which agrees with the results of Ref. 14 within the stated errors. The sum of the intensities of the 27 γ rays observed in this experiment has been normalized to 66 photons per 100 neutron captures following Refs. 3 and 4.

Peak number	E_γ (MeV)	$B_n - E_\gamma$	E_{ex} (MeV)	I_γ (photons/100 captures)		
				Present exp.	Ref. 4	Ref. 3
1	7.278	0.000	0.000	3.6	12.3	11
2	7.253	0.026	0.025	12.4		
3*	7.170	0.108	0.108	4.3	5.5	3.5
4*	7.071	0.207	0.207	10.4	9.1	5
5*	6.944	0.336	0.336	2.1	2.7	...
6*	6.799	0.479	0.479	2.9	2.5	3
7*	6.443	0.835	0.835	0.5	0.3	0.5
8*	6.117	1.160	1.161	1.7	2.1	1
9	6.045	1.233	1.233	<0.9		
10	5.932	1.346	1.345	0.4	0.8	0.5
11	5.785	1.493	1.481	0.3		
12*	5.772	1.506	1.504	1.1	1.7	1
13*	5.539	1.739	1.739	5.6	6	5
14	5.446	1.834	1.832	1.6	1.5	...
15	5.336	1.942	1.947	0.3		
16*	5.196	2.082	2.082	4.5	4.5	4
17	5.128	2.150	2.156	0.3		
18	5.086	2.192	2.192	1.8	9.3	7
19	5.045	2.233	2.231	0.7		
20	5.031	2.247	2.250	3.6	2.8	2
21	4.970	2.308	2.315	1.5		
22	4.934	2.344	2.359	0.5	3.2	2
23	4.898	2.390	2.388	0.3		
24	4.856	2.422	2.422	1.5	2.4	2
25	4.754	2.524	2.524	1.8		
26	4.722	2.556	2.545	0.4		
27*	4.593	2.685	2.685	1.3		

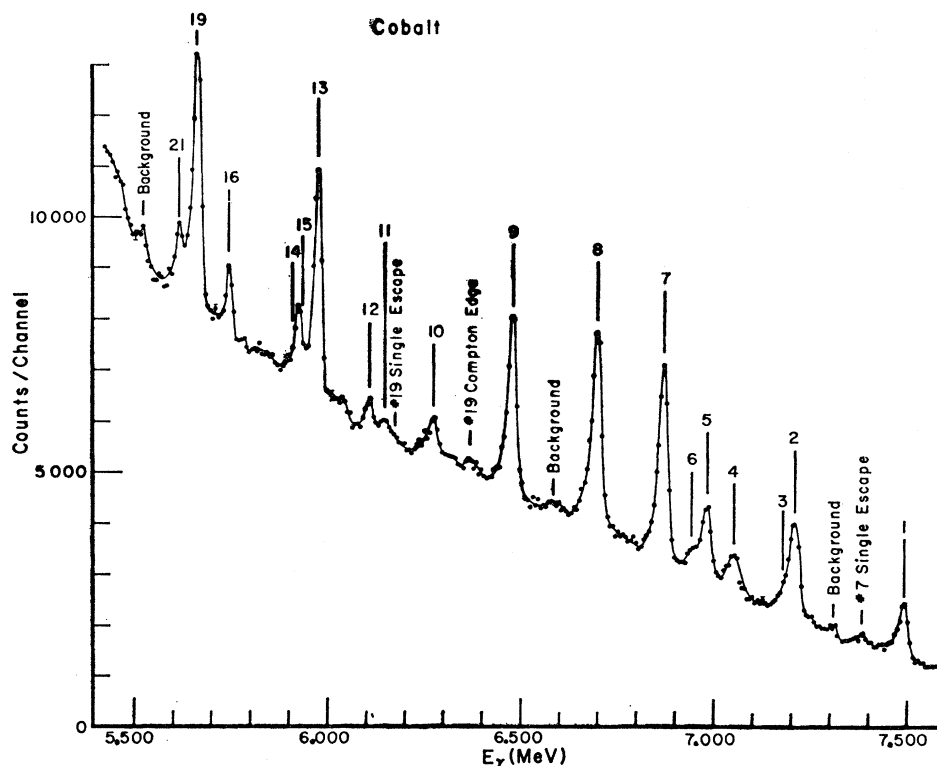


FIG. 13. Cobalt γ -ray spectrum observed with a gain of ~ 7 keV/channel.

strong contaminant group in the (d,p) study.¹⁸ The γ -ray intensities of earlier experimenters^{3,4} are also listed in the table.

Figure 12 diagrams the level energies measured in the (d,p) reactions.^{14,18} The γ rays measured in the present experiment and interpreted as initial transitions are also shown. It is evident that a number of (d,p)

levels exist for which no γ -ray transitions are observed. The present data show that, based on comparisons of absolute intensities from previous experiments, if such transitions exist they have intensities less than 0.1 photons per 100 neutron captures, except in the region $6.52 \text{ MeV} < E_\gamma < 6.59 \text{ MeV}$, where the upper limit is 0.25 photons per 100 neutron captures.

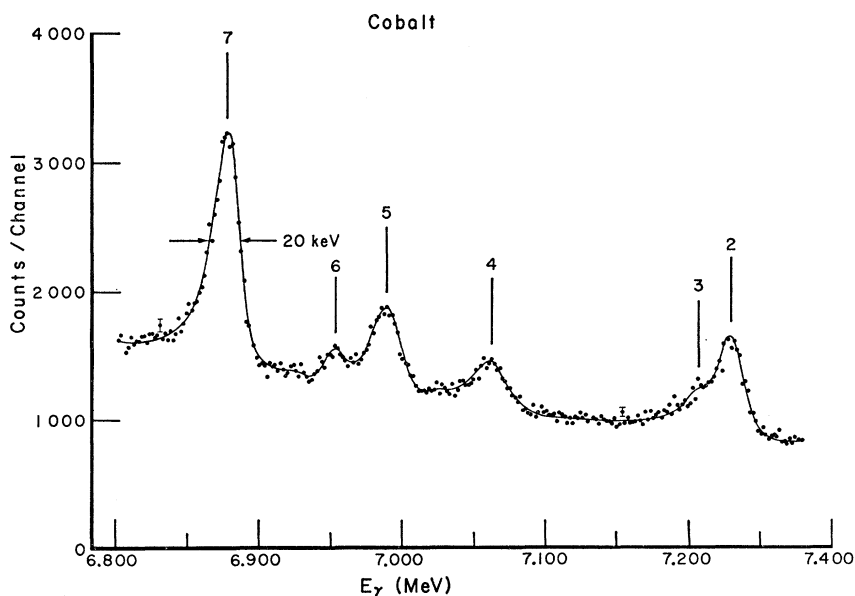


FIG. 14. Cobalt γ -ray spectrum observed with a gain of ~ 1.7 keV/channel for $6.80 \leq E_\gamma \leq 7.30$. The bump on the low energy side of peak 2 is the evidence for the existence of transition 3.

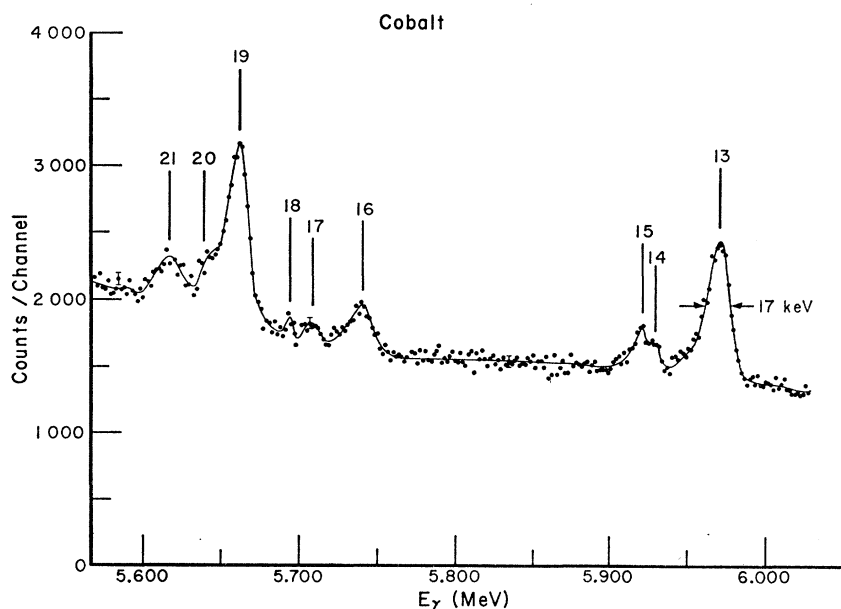


FIG. 15. Cobalt γ -ray spectrum observed with a gain of ~ 1.7 keV/channel for $5.60 \leq E_\gamma \leq 6.00$.

Cobalt

Sheets of cobalt metal of 99.9% purity were used to form a sample with a value of $n\sigma \sim 1.0$ in the standard geometry. The γ -ray spectrum shown in Fig. 13, obtained with a gain of 7 keV/channel, again showed the need for higher resolution. Figures 14 and 15 show the same energy region explored with a gain of 1.7 keV/channel.

Previous measurements^{3,4} have shown the existence of 12 lines in this region while the present work identifies at least 20 γ rays, possibly 21. The existence of line No. 3 is uncertain. Table IV lists the identification obtained in comparison with the (d,p) work.^{14,19} Sixteen transitions fit extremely well as initial transitions to known levels. The γ -ray energies of this experiment were determined using a neutron binding energy of 7.493 MeV.⁸

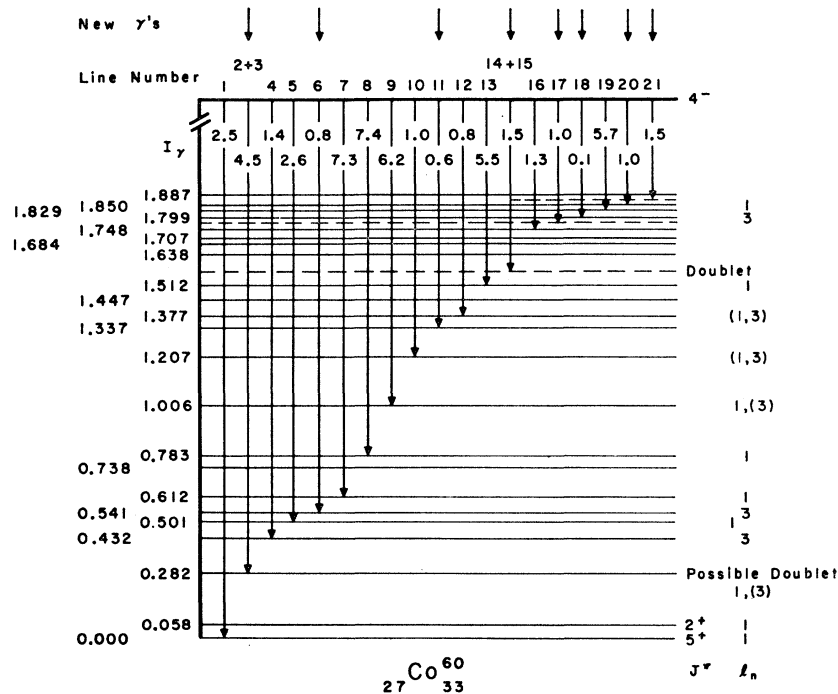


FIG. 16. Co^{60} energy level diagram. The excitation energies and values of I_n were taken from the (d,p) experiments of Refs. 14 and 19. The γ -ray transitions indicated by vertical lines are those observed in this experiment. The previously unreported transitions are noted by arrows at the top of the diagram. The sum of the 21 γ -ray intensities has been normalized to 52 photons/100 neutron captures following Refs. 3 and 4. The proposed new levels are indicated by dotted lines.

¹⁹ H. A. Enge, D. L. Jarrell, and C. C. Angelman, Phys. Rev. 119, 735 (1960).

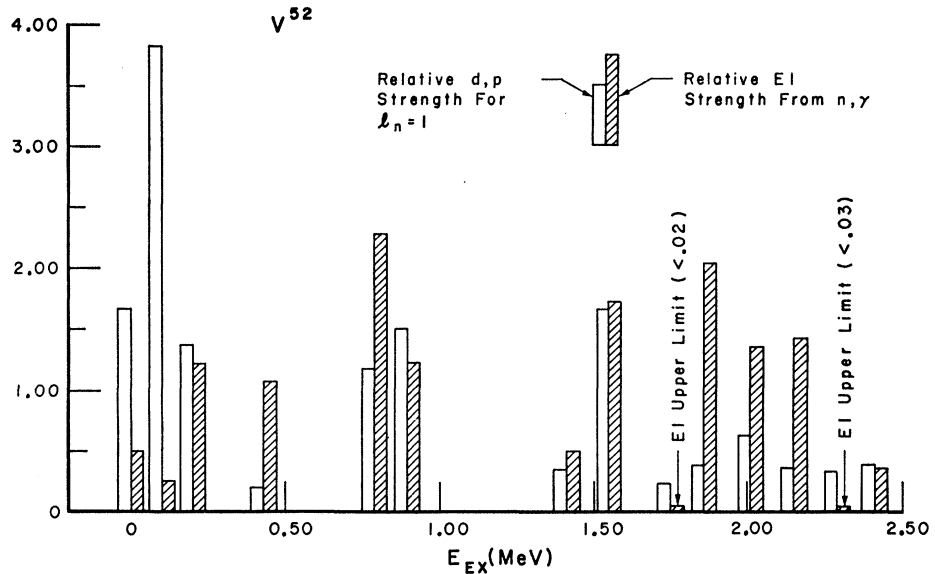


FIG. 17. Comparison of the reduced $E1$ strengths, I_γ/E_γ^3 , from the (n,γ) reaction with the (d,p) strengths, $(2J+1)S$, for those levels showing $l_n=1$ stripping patterns in vanadium. The strengths are in units relative to the average strengths for the 14 levels.

The level diagram shown in Fig. 16 illustrates the identification given in Table IV and shows the positions of the additional levels implied if all γ rays are interpreted as initial transitions. Again certain levels in the (d,p) reaction do not participate strongly in the (n,γ) reaction. The present data show that, if transitions to these levels exist, they have intensities less than 0.5 photons/100 neutron captures. Also there is no observed transition to the 58-keV first excited state.

DISCUSSION

Since the electromagnetic interaction is known, an evaluation of capture γ -ray intensities requires only knowledge of the structure of the capturing state and the final state. In the region of the periodic table of interest here, in favorable cases at least partial information on the final state is available from the value of l_n , the orbital angular momentum of the neutron transferred to that state in the (d,p) reaction. Even this knowledge, limited as it is, allows certain further information to be drawn from the capture experiments.

High resolution (d,p) angular distributions have been measured for V and Co by the M.I.T.^{13,19} group. For Mn, a (d,p) angular distribution has been measured with lower energy resolution by Dalton *et al.*²⁰ For excitation energies up to 3.03 MeV these authors measure 19 proton groups, 8 of which correspond to single levels resolved in the 90° measurements of Green *et al.*¹⁸

The shell model predicts low-lying p states for V, Mn, and Co, and a number of $l_n=1$ transitions are observed for each of these elements, as shown in Fig. 7, 12, and 16. These $l_n=1$ transitions are of particular interest in that they serve to locate states on which electric dipole

γ rays from the capturing state may be expected to terminate. Magnetic quadrupole components of such transitions, although allowed by the angular momentum selection rules, should be negligible.

Consider in detail the case of V. The multilevel analysis of Firk *et al.*¹⁵ of the total neutron cross sections shows that the state in which thermal neutrons are captured has important components from both the pos-

TABLE IV. Cobalt γ -ray energies and intensities. The asterisks in column 1 indicate the peaks used for energy calibration using a neutron binding energy B_n of 7.493 MeV from Ref. 8. Column 4 lists the excitation energy of the state populated by the primary γ -ray transition as determined from the (d,p) experiments of Ref. 19; these energies agree with the results listed in Ref. 14 within the stated errors. The sum of the 21 γ -ray intensities has been normalized to 52 photons per 100 neutron captures following Refs. 3 and 4. The existence of γ ray No. 3 is uncertain.

Peak number	E_γ (MeV)	$B_n - E_\gamma$	E_{ex} (MeV)	I_γ (photons/100 captures)		
				Present exp.	Ref. 4	Ref. 3
1	7.493	0.000	0.000	2.5	2.7	3
2*	7.211	0.282	0.282	3.7	4.4	4
(3)	7.190	0.303		<0.8		
4	7.059	0.434	0.432	1.4	...	1.3
5	6.989	0.504	0.501	2.6	3	2.5
6	6.949	0.544	0.541	0.8		
7*	6.881	0.612	0.612	7.3	8.8	7
8*	6.710	0.783	0.783	7.4	8.9	6
9*	6.487	1.006	1.006	6.2	6.5	5
10	6.281	1.212	1.207	1.0	1	0.8
11	6.150	1.343	1.337	0.6	9.8	0.6
12	6.110	1.383	1.377	0.8		
13*	5.981	1.512	1.512	5.5		
14	5.930	1.563		1.0		
15	5.921	1.572		0.5	6	2
16	5.740	1.753	1.748	1.3		
17	5.714	1.779		1.0	12.6	8
18	5.695	1.798	1.799	0.1		
19*	5.664	1.829	1.829	5.7		
20	5.642	1.851	1.850	1.0		
21	5.625	1.868		1.5		

²⁰ A. W. Dalton, G. Parry, H. D. Scott, and S. Swierszczewski Proc. Phys. Soc. (London) 78, 404 (1961).

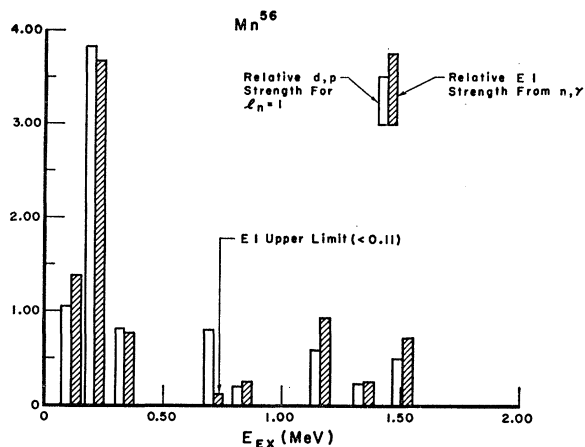


FIG. 18. Comparison of the reduced $E1$ strengths, I_γ/E_γ^3 , from the (n,γ) reaction with the (d,p) strengths $(2J+1)S$ for those levels showing $l_n=1$ stripping patterns in manganese. Only the 8 levels identified clearly as single levels in Ref. 20 are shown. The strengths are in units relative to the average strengths for the 8 levels.

sible spin values, 3^- and 4^- . Therefore, all states in V^{52} reached by $l_n=1$ have spins $(2^+, 3^+, 4^+, 5^+)$ which can also be reached by $E1$ radiation. It is seen by reference to the level diagram, Fig. 7, that the large majority of the γ rays observed in the present experiment do indeed terminate on $l_n=1$ levels. It is of course possible for $E1$ radiation to terminate in states which do not show the $l_n=1$ pattern. Thus, it is quite possible that all the observed γ rays in V are electric dipole in nature.

For electric dipole radiation it is instructive to calculate a reduced intensity, I_γ/E_γ^3 , which is proportional to $B(E1)$, the usual reduced-transition probability for electric dipole radiation. For the $l_n=1$ levels, this quantity, in units of its average value, is graphed in Fig. 17. It is seen that a variation in $B(E1)$ by a factor of 16 is observed in these γ rays. This is a small variation compared to the factor of 10^4 observed over the periodic table, but is probably limited by the intensity range of the present experiment.

Also obtainable from a plane-wave Born-approximation analysis of the (d,p) experiment¹³ are the relative transition strengths $(2J+1)S$, where S is the spectroscopic factor. If the capture process to every residual state proceeds via a simple direct single-neutron transition in the field of the target nucleus, the ratio of the (d,p) and (n,γ) transition strengths should be constant. Figure 17 shows that this is not the case.

For Mn , the measurements of Bernstein *et al.*²¹ of the capture of polarized neutrons by polarized Mn nuclei show that thermal-neutron capture is approximately equal for both spin states; this condition is incorporated in the multilevel analysis of Coté *et al.*²² Again, all the

states in Mn^{56} which can be reached by $l_n=1$ transitions can also be reached by electric dipole γ rays. Figure 18 shows that for seven of the eight levels resolved in the (d,p) reaction, the correlation between the strengths in (d,p) and (n,γ) is good. It is also clear that an improved (d,p) experiment would offer the opportunity for an unusually detailed test of the direct capture hypothesis because of the large number of resolved γ -ray transitions.

Turning to the Co data, it appears that the $J=4^-$ neutron resonance observed at 132 eV contributes about 80% of the thermal capture. Evidence for this is twofold: first, a calculation of the thermal capture cross section using the resonance parameters²³ in a single-level Breit-Wigner formula; second, the measurements of Schermer²⁴ with polarized neutrons on polarized Co . Consistent with this evidence is the observation of no change in the high-energy capture γ -ray spectrum between thermal and 132-eV neutron energies²⁵ along with the lack of any measurable γ -ray intensity to the $J=2^+$ first excited state at 58 keV (Fig. 16). If $J=3^-$ capture were also important one might expect an $E1$ transition of reasonable strength to the 58-keV level. For $J=4^-$ capture, magnetic quadrupole is the lowest multipole order allowed for a transition to the 2^+ state and is expected to be very weak.

Therefore if the Co thermal capture is dominated by the $J=4^-$ state, not all $l_n=1$ levels should be reached by electric dipole γ rays. Specifically $l_n=1$ levels with $J=2$ should not be populated. The levels for which $l_n=1$ is dominant in the stripping reaction¹⁹ are shown in Fig. 19. Again, a plane-wave Born-approximation analysis furnished the relative transition strengths, and again no unique proportionality between the (d,p) and

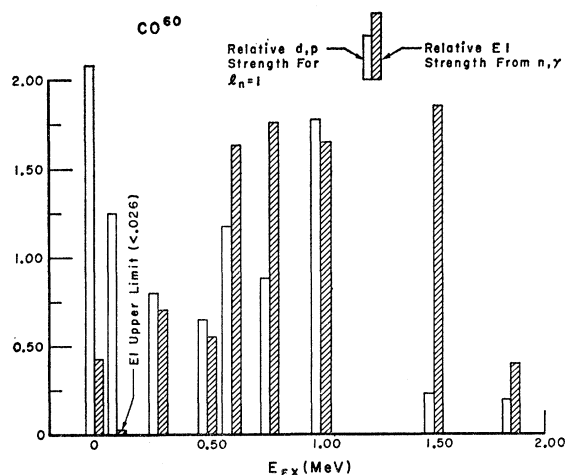


FIG. 19. Comparison of the reduced $E1$ strengths, I_γ/E_γ^3 , from the (n,γ) reaction with the (d,p) strengths, $(2J+1)S$, for those levels showing $l_n=1$ stripping patterns in cobalt. The strengths are in units relative to the average strengths of the 9 levels.

²¹ S. Bernstein, L. D. Roberts, C. P. Stanford, J. W. T. Dabbs, and T. E. Stephenson, *Phys. Rev.* **94**, 1243 (1954).

²² R. E. Coté, L. M. Bollinger, and G. E. Thomas, *Phys. Rev.* **134**, B1047 (1964).

²³ A. P. Jain, R. E. Chrien, J. A. Moore, and H. Palevsky, *Nucl. Sci. Eng.* **17**, 319 (1963).

²⁴ R. I. Schermer, *Phys. Rev.* **130**, 1907 (1963).

²⁵ O. A. Wasson and J. E. Draper (private communication).

(n,γ) strengths is observed. However, it may be noted that the variation in (n,γ) strength is less than a factor of 4, a fact which may reflect the restriction imposed by a unique spin of the capturing state.

Plots similar to Figs. 17, 18, and 19 have been given by Ikegami and Emery²⁶ for the even targets Fe⁵⁴ and Fe⁵⁶. They find, in the excitation region where seniority 3 states may be expected in the final nuclei, that the (d,p) levels are weak, corresponding to the fact that stripping reactions on these targets can excite only seniority 1 levels. Yet these levels are populated by strong γ rays; from this, these authors infer the influence of 3-particle "doorway states" in the region of the capturing state. In the present experiment it is quite likely that the V⁵¹ and Co⁵⁹ ground states are mixtures of seniority 1 and 3, in which case the (d,p) reaction can reach as high as seniority 4 in the residual odd-odd nucleus. The possible anticorrelation in (n,γ) and (d,p) strengths would be weakened in these cases.

In chlorine the low (d,p) states⁹ are predominantly $l_n=0$ and 2. In such cases the capture radiations are likely to be a mixture of compatible multipoles, and so more difficult to analyze. Draper and Fleischer¹⁰ have used (n,γ) intensities and branching ratios to infer spins and parities in the states of Cl³⁶ on the basis of theoretical single-particle transition rates. However, their assignments for the lowest states are questioned by Hoogenboom *et al.*⁹ who interpret their own stripping analysis in the light of the levels of the expected ground-state configuration. The two relatively weak new lines seen in the present experiment do not appear to afford

²⁶H. Ikegami and G. T. Emery, Phys. Rev. Letters 13, 26 (1964).

any enlightenment to the problem of the spin-parity assignments.

In conclusion it is useful to repeat that a distorted-wave Born-approximation analysis of a high-resolution (d,p) angular distribution for Mn would furnish a detailed case for comparison of (n,γ) and (d,p) intensities. The comparison of such results for the low states with levels in a similar region for V⁵² would be particularly interesting. The shell-model configuration for V⁵² is $(1f_{7/2})_p^{-3}(2p_{3/2})_n^{-1}$, while for Mn⁵⁶ it is $(1f_{7/2})_p^{-3}(2p_{3/2})_n^{-1}$. In the extreme of no configuration mixing the levels should be identical. It is clear from the level schemes that this extreme is not the case, but with knowledge of the values of l_n and the transition strengths interesting insights might be obtained.

Also interesting would be a distorted-wave Born-approximation analysis of the Co (d,p) data. If reliable absolute spectroscopic factors could be obtained, a unique opportunity to investigate the structure of the initial state could be afforded. Since the radiation width of the dominant 132-eV resonance is known, the measured (n,γ) intensities give the partial radiation widths directly. Given the important features of the final state from the (d,p) data, the single-particle components of the initial state might be ascertained.

ACKNOWLEDGMENTS

The authors acknowledge the assistance and suggestions of Barry Liles in fabricating the germanium detector. Discussions with Professor Howard L. Schultz were helpful and encouraging. Special thanks are expressed to Joseph Berti and Albert Nelson for the figures and to Miss Mary-Elizabeth Grady for typing the manuscript.